



CT-guided radiofrequency ablation of osteoid osteoma: correlation of clinical outcome and imaging features

Christoph Rehnitz, Simon David Sprengel, Burkhard Lehner, Karl Ludwig, Georg Omlor, Christian Merle, Hans-Ulrich Kauczor, Volker Ewerbeck, Marc-André Weber

PURPOSE

We aimed to retrospectively evaluate the computed tomography (CT) and magnetic resonance imaging (MRI) findings of patients with osteoid osteoma treated with CT-guided radiofrequency ablation (RFA) along with the clinical outcome and long-term success.

MATERIALS AND METHODS

Seventy-three CT-guided RFA procedures were performed in 72 patients. The long-term success was assessed using a questionnaire including several visual analog scale scores. The CT evaluation included pre- and immediate postprocedural imaging of all 72 patients, and MRI was performed in 18 patients with follow-up imaging (mean, 3.4±2.2 months). The evaluation criteria included nidus morphology and a correlation with markers of clinical success.

RESULTS

The primary technique effectiveness rate was 71/72 (99%). One relapse was successfully retreated, leading to a secondary technique effectiveness rate of 72/72 (100%). The long-term follow-up (mean, 51.2±31.2 months; range, 3–109 months) revealed a highly significant reduction of all assessed limitation scores ($P < 0.001$). The CT morphology was typical in all cases and did not change during the short-term follow-up. The follow-up MRI patterns varied considerably, including persistent nidus contrast enhancement in one-third (6/18) and persistent marrow edema in half (9/18) of the patients. None of the investigated MRI and CT patterns correlated with the clinical outcome.

CONCLUSION

The long-term outcome of CT-guided RFA of osteoid osteoma is excellent. There is no correlation of the CT and MRI patterns with the clinical outcome. Thus, the treatment decisions should not be solely based on the imaging findings. Investigators should also be aware of the variety of imaging patterns after RFA.

Osteoid osteoma (OO) is a benign bone tumor of childhood and adolescence (1–3), which typically causes severe bone pain that worsens during nighttime. In addition to conservative long-term treatment with nonsteroid anti-inflammatory drugs—which is problematic due to the side effects—the surgical resection of the nidus and several recently introduced minimally invasive therapies are treatment options for OO (4–6). Computed tomography (CT)-guided percutaneous radiofrequency ablation (RFA) has been the most commonly used method since its introduction in 1992 (7), with success rates of 67%–100% (8–11). Another promising technique is interstitial laser ablation (ILA). ILA can be performed using magnetic resonance imaging (MRI) guidance, thus preventing radiation exposure of the predominantly adolescent patients (12, 13). Minimally invasive thermal therapies have the potential to be cost-effective compared with open surgery (14). CT and MRI are typically used in the primary diagnostic work-up of OO, with CT being superior in the visualization of the nidus, and MRI being superior in the detection of the often extensive bone marrow edema (15). Pretherapeutic CT and MRI patterns are relatively well-known, but only a few studies have evaluated the post-therapeutic imaging changes. Lee et al. (16) reported that the ablation zone exhibited a target-like appearance with subsequent changes in the treated zone on standard MRI sequences. There is a lack of studies comparing the morphological imaging patterns, e.g., signal intensity and contrast enhancement of the nidus on MRI, with the clinical outcome.

Thus, our study has the following three purposes: to assess the clinical outcome of CT-guided RFA in OO, to evaluate the morphologic CT and MRI changes of OO pre- and postRFA, and to correlate imaging changes with markers of clinical success.

Materials and methods

Patient population

Institutional review board approval with a waiver of informed consent was obtained in this retrospective cohort analysis. Seventy-two patients who underwent 73 CT-guided RFA procedures for OO between January 2003 and January 2012 were included in the study.

Table 1 summarizes the study population and the clinical, CT, and MRI findings that were used to make the diagnosis. We did not routinely perform a biopsy prior to or during the RFA procedure in most cases (70 patients) because no histological confirmation prior to RFA is needed when the clinical and imaging features are suggestive of OO (17–19). Patients with an insufficient clinical history, with poor imaging quality (i.e., paper-printed images), who received treatments alternative to RFA

From the Departments of Diagnostic and Interventional Radiology (C.R. ✉ Christoph.Rehnitz@med.uni-heidelberg.de, S.D.S., H.U.K., M.A.W.), and Orthopedic Surgery (B.L., K.L., G.O., C.M., V.E.), University of Heidelberg, Heidelberg, Germany.

Received 15 October 2012; revision requested 15 November 2012; revision received 11 December 2012; accepted 15 December 2012.

Published online 8 March 2013
DOI 10.5152/dir.2013.096

Table 1. Overview of study population

		Result
Patients, n		72
Procedures, n		73
Age (years), median (range)		18 (3–68)
Gender, n (%)	Male	47 (65.3)
	Female	25 (34.7)
Follow-up time (months), mean±SD (median, range)		51.2±31.2 (49.00, 3–109)
Duration of symptoms prior to RFA (months), mean±SD (range)		15.7±19.9 (1–120)
Lesion location (n=72), n	Femur	26
	Tibia	24
	Humerus	7
	Spine	4
	Hip	3
	Radius	2
	Scapula	1
	Fibula	2
	Calcaneus	2
	Talus	1
Making of the diagnoses	Clinical presentation	Children, young adults
		Bone pain
		Worsening at night
		Pain relief under NSAID
	X-ray/CT/MRI	Radiolucent nidus
		+/- central calcification
		Cortical/subperiosteal bone formation
		Surrounding bone marrow edema
	Nuclear bone scan	Contrast-enhanced/T2-weighted-hyperintense nidus
		Focal enhancement in the early and late phases
Histological confirmation (n)	Double density sign	
	2 (DD, Brodie's abscess)	

CT, computed tomography; DD, differential diagnosis; MRI, magnetic resonance imaging; NSAID, nonsteroidal anti-inflammatory drugs; OO, osteoid osteoma; RFA, radiofrequency ablation; SD, standard deviation.

both before and after the treatment. Thus, 18 patients were included in the MRI evaluation.

RFA technique

General information about the RFA technique is provided in previous studies (7–9, 20–24). The specific technical considerations used in our study are as follows: The procedure was performed under general (70 patients) or spinal (two patients) anesthesia. In our opinion, local anesthesia does not provide sufficient pain control, especially when entering the nidus and during the ablation. Anesthesiologists and the patients themselves decided between spinal and general anesthesia. However, because the complication rates are comparable overall in young and otherwise healthy patients for both methods, general anesthesia was most commonly performed. A thin-sliced (maximum slice thickness, 2 mm; range, 0.6–2 mm) CT scan was performed, covering the nidus and the minimum caudal and cranial extent needed for planning safe bone access. Bone access and nidus penetration was performed with different devices; the Bonopty system (Bonopty®, AprioMed, Uppsala, Sweden) was used most often. The radiofrequency electrode (Cool-tip™, Valleylab, Tyco Healthcare Group LP, Boulder, Colorado, USA) was then inserted, and the active tip (7 or 10 mm active tip) was placed within the nidus.

Multiplanar reconstructions were used to optimally position the active tip. The ablation was then performed, reaching a target temperature of 90°C for a total ablation time of 400 s.

Effectiveness of technique and long-term outcome

Primary and secondary effectiveness of technique were defined according to the SIR guidelines (25) as successful treatment either within the initial ablation or after a repeated ablation, respectively. A radiologist and an orthopedic surgeon performed the initial postinterventional assessment during a clinical examination before the patient was discharged. Follow-up examinations were typically performed three months after the RFA.

or who were treated with RFA for tumors other than OO were excluded from this study. Of the 73 OO patients, one patient was excluded due to poor imaging quality and missing clinical data.

For the outcome evaluation, we included all 72 patients with OO treated with CT-guided RFA and fully available clinical data (see also the imaging section). For the imaging evaluation, we included only those patients who underwent both pre- and post-ther-

apeutic imaging. All the patients had a CT scan immediately after the RFA procedure to exclude complications. The patients also had CT scans of only the nidus before the procedure to serve as an initial comparison exam, making complications easier to detect. Thus, all 72 patients were included in the CT evaluation. Overall, 51 MRI examinations (either performed before [n=27] or after [n=24] the RFA) were available. Only 18 patients had MRIs available

The long-term outcome was qualitatively and quantitatively assessed using a standardized questionnaire that was mailed to all patients at the end of the patient inclusion period, with a time interval of at least three months after the RFA. The questionnaire comprised 35 questions divided into a pre- and a postRFA section, including personal, social, and clinical problems and subjective changes following the RFA. Key questions were the severity of pain (night pain, daily pain, stress-related pain) assessed with a visual analog scale

(VAS) from 0 (no pain) to 10 (worst imaginable pain) and patient satisfaction (from “completely not” to “limited” to “mostly and very satisfied”). We defined a reduction of >30% in the VAS score, no pain medication, and a patient satisfaction of at least “mostly satisfied” with a minimum time interval of three months after the RFA as long-term success (26). Failure was defined as the lack of significant pain reduction/persistent pain or a patient satisfaction worse than “mostly satisfied”. Further questions quantitatively assessed the limitations

in daily and sports activities, the time to pain relief and the occurrence of any complications. If patients could not be contacted via mail or if answers were equivocal, we again contacted them by phone to obtain all questionnaire data. The patients were instructed to contact our department in case of pain recurrence or other complications. Major complications were defined as an event that leads to substantial morbidity and disability, increase in the level of care, or hospital admission or a substantially lengthened hospital stay (25).

Table 2. Imaging protocol, scanner, and analysis

	Available imaging		Imaging analysis
CT		CT	
Number of evaluations	72 patients with follow-up imaging 73 procedures (one relapse) 146 CTs	Nidus size	a×b
System	Siemens Somatom Sensation 16 ^a (34 patients, 68 CTs) Philips MX 8000 ^b (38 patients, 78 CTs)	Nidus volume	a×b×c×0.52
Parameters (minimally required)	Maximum 2 mm slice thickness covering region of interest Kernel: bone Window: bone	Nidus calcification	Yes/No
		Cortical thickening Location within the bone	Marked/Slight/No Subperiosteal, cortical, medullary
MRI		MRI	
Number of evaluations	18 patients with follow-up imaging 36 MRIs (in addition to the CT-scans pre- and postRFA)	Sequence	Nidus morphology pre- and postRFA
PreRFA	12 Verio ^a (3.0 T) 3 Intera ^b (1.0 T) 1 Sonata ^a (1.5 T) 1 Aera ^a (1.5 T) 1 Avanto ^a (1.5 T)	T1-weighted, T2-weighted	Hypo-, iso-, hyperintense compared with the surrounding muscle
PostRFA	15 Verio ^a (3.0 T) 3 Intera ^b (1.0 T)	T1-weighted CE	- no enhancement + slight/moderate ++ strong
Parameters (3.0 T Verio ^a)	T1-weighted (TR/TE, 728/12) Coronal STIR (TR/TE, 2890/39; TI, 210) Sagittal T2-weighted (TR/TE, 3740/92) Axial T2-weighted (TR/TE, 4750/72) with fat suppression Axial (TR/TE, 945/11) Coronal T1-weighted (TR/TE, 728/12) after i.v. administration of gadoterate-meglumine (0.1 mmol per kilogram of body weight, Dotarem; Guerbet, Villepinte, France)		Extent of surrounding bone marrow edema
		STIR	- no edema + slight/moderate edema ++ strong edema

^aSiemens, Erlangen, Germany.

^bPhilips Medical Systems, Best, the Netherlands.

CE, contrast-enhanced; CT, computed tomography; MRI, magnetic resonance imaging; RFA, radiofrequency ablation; STIR, short tau inversion recovery; T, Tesla; TE, echo time; TI, inversion time; TR, repetition time.

Imaging evaluation

CT

As shown in Table 2, all 72 patients had CT imaging available before and immediately after the procedure. Including the one relapse that was re-treated, a total of 73 RFA procedures were performed. Thus, all CT scans (n=146), performed on two different multidetector CT scanners, were evaluated. The images were evaluated for location, size, and volume of the lesion, presence or absence of calcification and cortical thickening. The same parameters were re-evaluated after the treatment.

MRI

Details about the scanners, imaging protocols, and image evaluation protocol are summarized in Table 2. We analyzed 18 patients who received MRI scans before and after the treatment (altogether 36 examinations). As with other experienced groups (9), the recommendation for an MRI was made after discussion of the case in an interdisciplinary team based on the certainty of the diagnosis (clinical, CT, and nuclear bone scan results). In the postoperative setting, we routinely recommended a follow-up MRI under the assumption that the nidus and surrounding bone marrow morphology might be evaluated superiorly. Despite our advice, some patients did not receive follow-up MRI exams. Follow-up imaging was usually performed during the clinical 3–6 months follow-up. The mean follow-up time was 3.4±2.2 months (range, 0–10 months). The majority (27/36 examinations) were examined using a 3.0 Tesla system (Magnetom Verio, Siemens, Erlangen, Germany). We also included images from other 1.0 and 1.5 Tesla scanners. All these examinations were of diagnostic quality and included standard sequences as the minimal requirement: T1-weighted spin-echo/turbo spin-echo (SE/TSE), T2-weighted TSE, short tau inversion recovery (STIR), and T1-weighted SE/TSE after the intravenous injection of a contrast agent.

Because we included different magnetic field strengths, we refrained from a quantitative evaluation. We instead focused on a basic visual evaluation: presence/absence of marrow edema, signal intensity of the nidus

(hypo-, iso-, or hyperintense compared with the surrounding muscle tissue), contrast enhancement of the nidus (strong/moderate/absent). Additional MRI examinations that were performed because of other indications, such as long-term follow-up, persistent nidus enhancement or patient request, were not included as part of the pre- or postRFA MRI evaluations. The entire imaging data sets were available in DICOM format on our picture archiving and communication system (PACS, GE Centricity Enterprise™, Version 4.2.7.4, General Electric Healthcare Pty Ltd., Piscataway, New Jersey, USA) and analyzed in consensus by two experienced radiologists with eight and ten years of experience in this area. To avoid any bias of reading the two different modalities, the CT and MRI images were subdivided and analyzed separately with a minimal time interval of seven days between the CT and MRI assessments.

Correlation of outcome with imaging patterns

All assessed CT and MRI patterns were correlated with the different VAS scores using the Pearson correlation to depict positive or negative correlations of any imaging patterns with the clinical outcome.

Data analysis and statistics

Descriptive statistics (mean, standard deviation, range, median) were provided where appropriate (e.g., pre- and post-therapeutic imaging changes and clinical symptoms). Parametric data (e.g., changes postRFA in the nidus size/volume or VAS score) were tested using a two-tailed Student's *t* test. Morphologic imaging findings were compared with several items of the questionnaire, e.g., the clinical outcome assessed with the VAS pain score as its main surrogate parameter.

Pre- and postRFA variables (e.g. day pain, night pain) were compared using nonparametric tests. Correlations were assessed using Pearson's correlation coefficients: pain reduction (delta VAS score) vs. (a) nidus location (spinal, various extremity bones, intra-/periarticular), (c) nidus calcification, (d) marrow edema, (e) T2-weighted intensity/contrast enhancement, and nidus vol-

ume vs. night pain, intra-/periarticular location and limitations in daily activity. Correlations between the measurement of the nidus volume using MRI or CT (both pre- and postprocedural) were also tested using Pearson's correlation coefficients. Coefficients higher than 0.5 indicate a moderately positive correlation (27). Correlations between categorical data (e.g., lesion location, gender) were evaluated with the chi-square test. A *P* value of less than 0.05 was considered significant. The data analysis and statistical evaluation were performed using a commercially available software (Statistical Package for Social Sciences, version 18, SPSS Inc., Chicago, Illinois, USA).

Results

Effectiveness of technique and long-term outcome

The follow-up time of the 72 OO patients was 3–109 months (mean, 51.2±31.2 months; median, 49 months). The primary technique effectiveness was 71/72 (99%). Although all other patients remained symptom-free during the follow-up period, one patient with an OO in the femur developed a relapse 14 months after the RFA. The RFA was successfully repeated with no signs of a further relapse until the final follow-up. Thus, the secondary technique effectiveness rate was 72/72 (100%).

The patients described several significant personal limitations caused by the OO. The highest score was reported regarding the night pain, but other limitations, such as day-time pain, taking medication, limitations regarding sports and daily activities, and effect on performing the job or educational requirements, also had a significant impact. The details are presented in Fig. 1, which also demonstrates the development of those limitations after the RFA. A distinct reduction (*P* < 0.001 for all items) in the VAS scale (0–10, with 0=no pain/limitation up to 10=maximum pain/limitation) was found for all assessed limitation scores. After the RFA, the pain usually resolved within a week, although a delayed resolution was reported in 27% of the cases. One patient, however, reported experiencing pain for a period of four months. Additionally, 92% were “very satisfied”

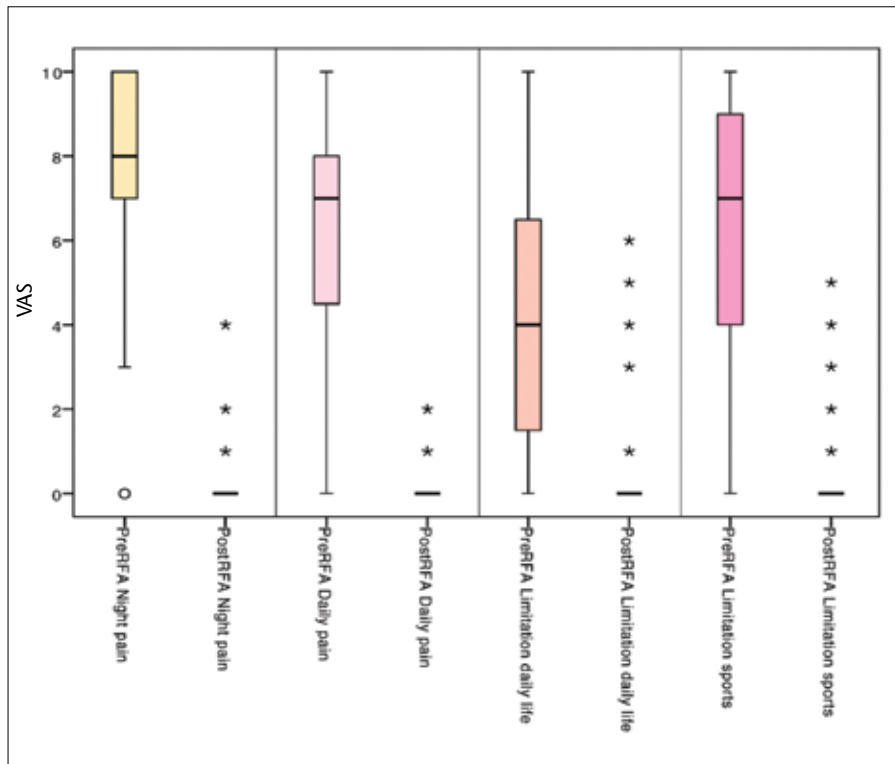


Figure 1. Effectiveness of RFA regarding factors that negatively affect the quality of life. The bar graphs demonstrate the subjective rating of several factors negatively affecting the quality of life by the osteoid osteoma patients before and after the RFA based on a visual analog scale (VAS), which ranged from 0 (no pain/relevance) to 10 (worst imaginable pain/most relevant). Before the RFA, the scores were high for night pain, day pain and limitations in sports activity and moderate for limitations of daily life. The effectiveness of the RFA was demonstrated by a highly significant reduction of the different scores after the RFA ($P < 0.001$ for all items), reaching normal or almost normal values. The asterisks represent the few outliers.

with the procedure and outcome, and the remainder were “satisfied”. No major complication occurred. A 1 cm² skin area of hypoesthesia around the surgical access path was reported by one patient three weeks after the RFA and was rated as a minor complication. However, the hypoesthesia completely resolved, resulting in a symptom-free eight month follow-up. The questionnaire was completed by 56/72 (77.8%) patients. Eight patients who did not respond were secondarily contacted by phone and provided basic information: none reported any remaining symptoms, complications, or relapses requiring further treatment.

Imaging findings

CT patterns and correlation with clinical outcome

We evaluated 146 CT scans of the 73 procedures in 72 patients. The mean nidus size was 5.5×5.4×7.4±2.49×2.56×2.55 mm³ (x-, y-, and z-axis, respectively), with a min-

imum/maximum diameter of 1/14 mm. The mean nidus volume was 0.16±0.24 cm³ (range, 0.01–0.93 cm³). An excellent correlation was found between the measurement of the nidus volume using MRI and CT ($r=0.844$, $P < 0.01$). The nidus was located at the cortex in 54.2% (39/72), within the subperiosteum in 16/72 (22.2%), and in the bone marrow in 17 cases (23.6%). A marked cortical thickening was present in 43/72 (59.7%) patients, four patients showed slight thickening, and 25 patients showed no cortical thickening. Nidus calcification was found in 56/72 (77.8%) patients. The patient who developed a relapse with severe local pain 14 months after RFA showed similar patterns before and after the treatment. A small hypodense nidus surrounded by cortical thickening was present both before the RFA and at the point of relapse. No calcification of the nidus was visible. A moderate negative correlation was found between the nidus volume

and the preprocedural pain ($r=-0.34$, $P = 0.015$). No significant correlations were found between the nidus volume and (1) night pain after RFA ($r=0.07$, $P = 0.6$), (2) day pain ($r=0.20$, $P = 0.15$), (3) sports activity ($r=0.17$, $P = 0.90$), and (4) daily activity ($r=0.09$, $P = 0.52$). Additionally, no significant correlation was found for any other CT pattern. Fig. 2 demonstrates the typical CT patterns of an OO patient and the details for the RFA procedure.

MRI patterns and correlation with clinical outcome

We evaluated 36 pre- and postprocedural MRI examinations from 18 patients. The mean follow-up time was 3.4±2.2 months (range, 0–10 months or 1–323 days). The most common, and thus considered typical, MRI morphology is demonstrated in Fig. 3. The detailed results from the imaging analyses are provided in Table 3 and Fig. 4, where the imaging patterns and frequencies before and after the RFA are presented. The principal signal pattern prior to the RFA was isointensity on T1-weighted images (14/18, 78%), hyperintensity on T2-weighted images (16/18, 89%), and strong contrast enhancement (18/18, 100%). The nidus was surrounded by marked marrow edema in 15/18 patients (83%). The postRFA T1-weighted and T2-weighted images were more inhomogeneous but showed larger fractions of hypointensity for both. No visible contrast enhancement was noted at follow-up in most cases (12/18), but 6/18 patients showed diminished and somewhat persistent enhancement (Fig. 5). The surrounding bone marrow edema was also reduced or absent in all patients, persisting partially in 9/18 patients. This reduction coincided with a marked decrease in the VAS pain score. The median baseline score was 8 (range, 6–10; mean, 8.1±2.2) preRFA and 0 (range, 0–4; mean, 0.27±0.68) postRFA. The only patient with a relapse presented with local severe pain 14 months after a successful RFA. MRI at the point of relapse revealed a contrast-enhanced T2 hyperintense nidus and surrounding marrow edema. RFA was repeated, and further clinical follow-up was unremarkable.

Table 3. Results from MRI before and after the RFA

Patient	PreRFA				PostRFA				Follow-up	
	T1-weighted	T2-weighted	Contrast-enhanced	Edema	T1-weighted	T2-weighted	Contrast-enhanced	Edema	Months	Days
1	Isointense	Hyperintense	++	++	Isointense	Hyperintense	+	-	5	168
2	Hypointense	Hyperintense	++	++	Hypointense	Isointense	+	+	2	69
3	Isointense	Hyperintense	++	++	Isointense	Hypointense	+	++	0	1
4	Isointense	Hyperintense	++	++	Isointense	Hyperintense	-	+	5	177
5	Isointense	Hyperintense	++	++	Hypointense	Hypointense	-	-	4	135
6	Isointense	Hyperintense	++	++	Isointense	Hyperintense	+	+	4	132
7	Isointense	Hyperintense	++	++	Isointense	Isointense	-	+	3	100
8	Isointense	Hyperintense	++	++	Hypointense	Hypointense	-	+	0	16
9	Isointense	Hyperintense	++	+	Hypointense	Hyperintense	-	+	3	92
10	Isointense	Isointense	++	++	Hypointense	Hypointense	-	-	3	94
11	Hypointense	Isointense	++	++	Hypointense	Hypointense	-	+	2	73
12	Isointense	Hyperintense	++	+	Isointense	Hypointense	-	-	4	135
13	Hypointense	Hyperintense	++	++	Isointense	Hypointense	+	+	5	171
14	Hyperintense	Hyperintense	++	++	Hypointense	Hypointense	+	-	2	84
15	Isointense	Hyperintense	++	++	Isointense	Hypointense	-	-	3	107
16	Isointense	Hyperintense	++	++	Hyperintense	Hypointense	-	-	10	323
17	Isointense	Hyperintense	++	++	Isointense	Hypointense	-	-	3	94
18	Isointense	Hyperintense	++	+	Hypointense	Hypointense	-	-	3	107
Mean									3.4	115

++, strong; +, slight/moderate; -, absent.

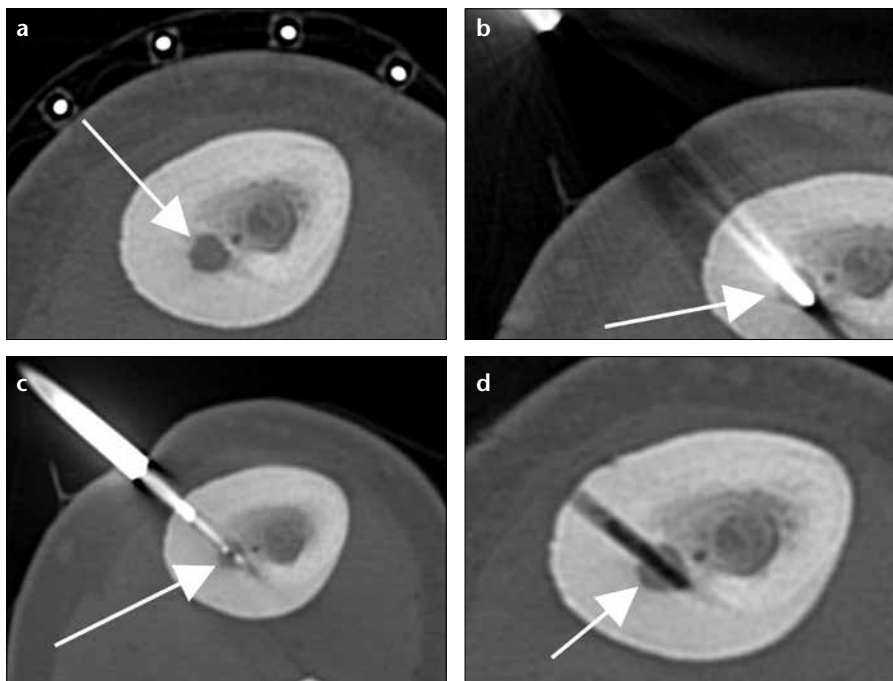


Figure 2. a–d. CT morphology and RFA procedure. Axial CT (a) demonstrates the cortically located nidus (arrow) leading to a marked surrounding subperiosteal/cortical thickening. Due to the marked cortical thickening, a power drill (b) was used for bone access, and the nidus was centrally penetrated (arrow). The active tip (c, arrow) of the ablation electrode was placed centrally into the nidus. CT after the procedure (d) shows the access way but no change in the size or morphology of the nidus itself (arrow).

Discussion

We present a comparatively large series of 72 OO patients treated with CT-RFA, which was evaluated regarding the outcome, imaging features, and possible correlations between these parameters.

In our study, we achieved a high primary technique effectiveness rate of 99% (71/72 patients) within one procedure and a secondary technique effectiveness rate of 100% (72/72) after repeated RFA due to a relapse. A lower primary technique effectiveness of 67%–79% has been reported (10, 28–31). The more recent studies report comparable primary technique effectiveness of 85%–100% (32–35). One factor leading to the high success and low relapse rate in our study might be the longer ablation time compared with some previous studies (10), which is corroborated by the data of other studies with similar findings (24).

The long-term outcome (mean follow-up time, 51.2 months; range,

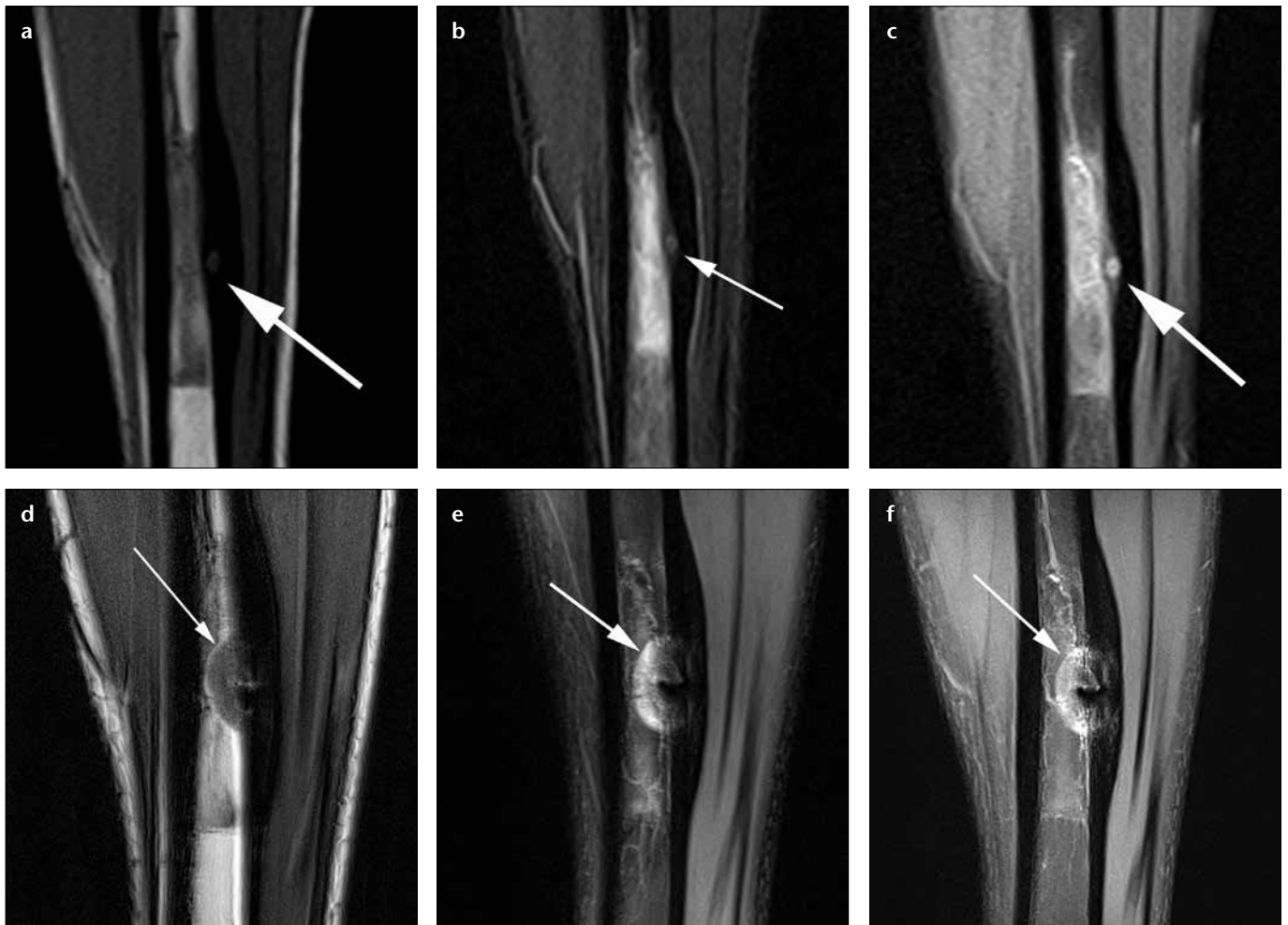


Figure 3. a–f. MRI patterns before and after the RFA. Pretherapeutic coronal T1-weighted (a), T2-weighted fat-suppressed (b), and contrast-enhanced fat-suppressed T1-weighted (c) MR images show T1-weighted isointense and T2-weighted hyperintense patterns and a strongly contrast-enhanced pattern of the nidus compared with the surrounding muscles (a–c, arrows). Note also the reactive enhancement/edema of the bone marrow. Coronal MRI after the RFA demonstrates, compared with the muscle tissue, T1-weighted isointense (d), T2-weighted hyperintense (e), and contrast-enhanced (f) patterns of the ablation area but no visible enhancement within the area of the former nidus (d–f, arrows).

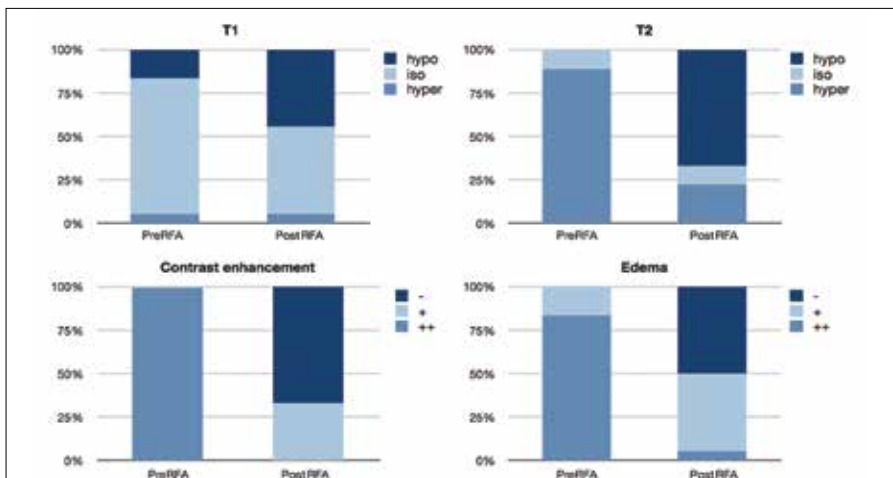


Figure 4. Signal intensities before and after the RFA. The bar graphs show the proportion of the different signal intensities of the nidus in T1-weighted, T2-weighted, and contrast-enhanced T1-weighted MR images as well as the presence and extent of the surrounding bone marrow edema in 18 patients at the baseline and follow-up MRI examinations. Before the RFA procedure, the nidus signal intensities were estimated as mostly T1-weighted hypointense, T2-weighted hyperintense, and contrast-enhanced with a marked surrounding marrow edema. The follow-up MRI patterns varied more, with larger proportions of hypointensity on T1-weighted/T2-weighted MR images, and a reduced but partly persistent contrast enhancement of the nidus and bone marrow edema.

3–109 months), as assessed with a questionnaire that was mailed to all patients at the same time point, was excellent. We found a highly significant reduction in the VAS scores regarding all evaluated outcome parameters ($P < 0.001$ for all items). This result demonstrates the effectiveness of RFA with respect to not only pain relief but also all other factors that negatively impact the quality of life, such as limitations in performing the job/educational requirements or sports activities. These results also support the previous findings of Barei et al. (36), who investigated similar items in a small series of patients.

Our relatively uniform CT and pre-procedural MRI patterns were in agreement with the literature (16, 37–42), but the follow-up (mean, 3.4 ± 2.2 months) MRI varied considerably. In

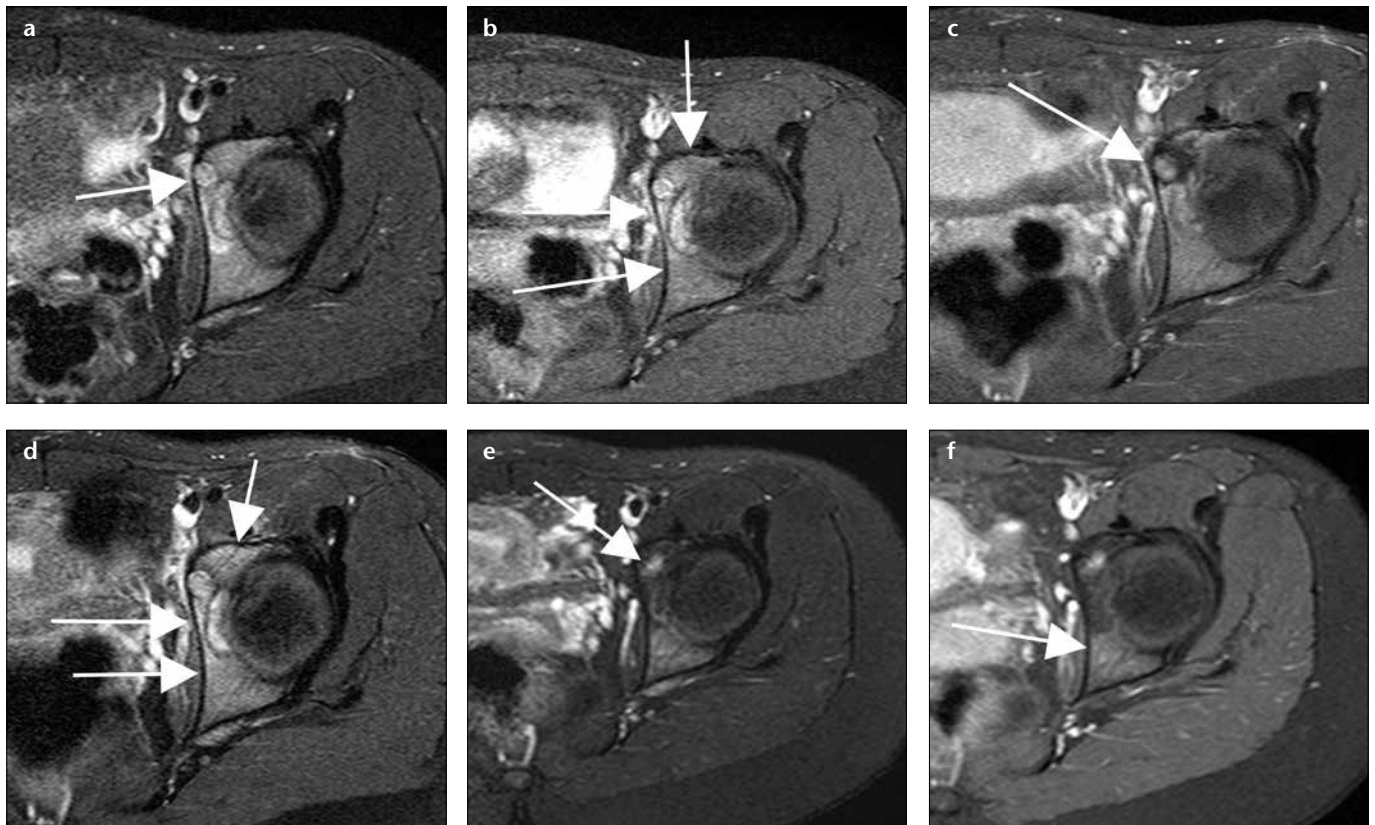


Figure 5. a–f. Atypical MRI patterns: persistent contrast enhancement and bone marrow edema. Baseline and follow-up imaging in contrast-enhanced fat-suppressed T1-weighted and T2-weighted fat-suppressed images, MR images, respectively. On the baseline contrast-enhanced fat-suppressed T1-weighted image (a), a contrast-enhanced nidus is present in the medial anterior aspect of the left acetabulum (arrow). A marked bone marrow edema surrounds the nidus (b, arrows) on the T2-weighted fat-suppressed images. On three-month follow-up, the nidus shows a centrally persistent contrast enhancement on the contrast-enhanced fat-suppressed T1-weighted image (c, arrow) and a partly persistent marrow edema (d, arrows) on the T2-weighted fat-suppressed image. On thirteen-month follow-up, visible partial persistence of the nidus enhancement in the contrast-enhanced fat-suppressed T1-weighted image (e, arrow) and marrow edema in the T2-weighted fat-suppressed image (f, arrow) remain.

general, the contrast enhancement of the nidus was reduced in all patients, the preprocedural T2-weighted hyperintense pattern changed after the RFA towards iso- or hypointensity, and the surrounding marrow edema was diminished. In contrast to those expected patterns, one-third (6/18) of the patients showed a partially persistent nidus contrast enhancement, and half of the patients (9/18) showed surrounding marrow edema. In contrast to our more heterogeneous postprocedural MRI findings, Lee et al. (16) described uniform patterns with a non-enhanced, T2-weighted hypointense central zone at the two-month follow-up in 16/16 patients. Afterwards, the signal patterns changed, leading to an enhanced nidus in all cases (16).

None of the CT or MRI patterns correlated with the clinical outcome. All patients reported a highly significant reduction in the VAS pain score as the

key clinical outcome parameter regardless of the MRI/CT morphology. Thus, neither pre- or postprocedural nidus size nor location or nidus morphology should influence the therapy decision-making or be used as an outcome predictor. This result is supported by the data of Vanderschueren et al. (37), who found that the nidus size was not correlated with unsuccessful coagulation. PostRFA MRI changes that are supposed to indicate healing (decrease in contrast enhancement, diminished/vanished edema) were accompanied by a marked reduction in the VAS pain score. The general decrease in the VAS pain score along with the decrease in the contrast enhancement of the nidus might be an expression of healing/treatment success. Therefore, the follow-up MRI might be useful and could additionally be used as a postoperative basis for further follow-up in cases of relapsing symptoms. Our hypothesis

on the symptoms of a relapse would be an increase in the VAS pain score accompanied by an increase in the contrast enhancement visualized by MRI. To prove this hypothesis, a prospective study with a quantitative assessment of the enhancement and the inclusion of relapsed patients would be desirable. However, our findings show that even a persistence of those signs of potential activity (edema, contrast enhancement) are not necessarily correlated with the clinical symptoms, thus supporting the previous findings of Vanderschueren et al. (37), who described a persistent “edema-like” pattern in 5/5 unsuccessfully treated patients and also in 9/13 successfully treated patients.

Practically, our data support the following uses of the imaging modalities in the management of OO: 1) In the primary diagnosis, both CT and MRI show typical patterns and, in unclear

cases, may be used complementarily, e.g., to compare the patterns with other relevant differential diagnoses such as Brodie's abscess (43). 2) In the follow-up scenario, typical and expected MRI patterns include reductions in the nidus enhancement and bone marrow edema accompanied by a marked reduction in pain. Thus, if performed, a comparison of the pre- and postprocedural MRIs might be useful. However, the persistence of edema and nidus enhancement is within the normal range, and in the absence of pain, they are not predictors of a relapse. In this scenario, MRI follow-up is of limited value, and the variety of imaging patterns must be kept in mind. 3) The situation becomes more difficult in cases presenting with persistent pain. Our only patient with a relapse showed a marked nidus enhancement and surrounding edema, which makes sense in light of the morphology of the vital nidus before the RFA. There is a good likelihood that the coincidence of pain and nidus enhancement hints at a relapse, and thus rRFA should be considered under those conditions. If no enhancement can be observed, other reasons for pain, e.g., complications, should be suspected. To test this last hypothesis, additional studies investigating cases with postprocedural pain would be desirable.

The present study had several limitations. One limitation is the retrospective study design with RFA as a single therapy modality. The success rates were compared with reports on other procedures, although a prospective comparison of RFA and promising techniques such as ILA or microwave ablation would be desirable. Not all patients answered our questionnaire, and some were lost to follow-up; however, a response rate of 77.8% is comparably high (44). Additionally, we increased the overall response rate by contacting eight additional patients who provided basic information. As RFA is a very effective method and as there was only one case that failed, the assessment of the conditions and imaging signs that led or coincides with treatment failure is limited. Additionally, not all patients were examined using the same field strengths. Thus, only the evaluation of basic imaging patterns

and changes was possible. A prospective study design using the same MRI system and sequence protocol would overcome this limitation and would allow for additional quantitative analyses of the nidus enhancement.

In conclusion, the long-term outcome of CT-guided RFA is excellent. None of the CT and MRI patterns showed a relevant correlation with the clinical outcome. An MRI may not be necessary during routine follow-up but could serve as basic postoperative imaging to detect nidus changes early in cases when the symptoms of a relapse may be present. When performed, investigators should be aware of the variety of imaging patterns and should not initiate further treatment decisions that are solely based on imaging.

Conflict of interest disclosure

The authors declared no conflicts of interest.

References

1. Gangi A, Alizadeh H, Wong L, Buy X, Dietemann JL, Roy C. Osteoid osteoma: percutaneous laser ablation and follow-up in 114 patients. *Radiology* 2007; 242:293–301. [\[CrossRef\]](#)
2. Motamedi D, Learch TJ, Ishimitsu DN, et al. Thermal ablation of osteoid osteoma: overview and step-by-step guide. *Radiographics* 2009; 29:2127–2141. [\[CrossRef\]](#)
3. Unni KK, Dahlin DCB. Dahlin's bone tumors: general aspects and data on 11 087 cases. Philadelphia: Lippincott-Raven; 1996.
4. Gangi A, Dietemann JL, Gasser B, et al. Interventional radiology with laser in bone and joint. *Radiol Clin North Am* 1998; 36:547–557. [\[CrossRef\]](#)
5. Sans N, Galy-Fourcade D, Assoun J, et al. Osteoid osteoma: CT-guided percutaneous resection and follow-up in 38 patients. *Radiology* 1999; 212:687–692.
6. Laus M, Albisinni U, Alfonso C, et al. Osteoid osteoma of the cervical spine: surgical treatment or percutaneous radiofrequency coagulation? *Eur Spine J* 2007; 16:2078–2082. [\[CrossRef\]](#)
7. Rosenthal DI, Alexander A, Rosenberg AE, et al. Ablation of osteoid osteomas with a percutaneously placed electrode: a new procedure. *Radiology* 1992; 183:29–33.
8. Bruners P, Penzkofer T, Gunther RW, et al. Percutaneous radiofrequency ablation of osteoid osteomas: technique and results. *Rofo* 2009; 181:740–747. [\[CrossRef\]](#)
9. Hoffmann RT, Jakobs TF, Kubisch CH, et al. Radiofrequency ablation in the treatment of osteoid osteoma: 5-year experience. *Eur J Radiol* 2010; 73:374–379. [\[CrossRef\]](#)

10. Kjar RA, Powell GJ, Schlicht SM, Smith PJ, Slavin J, Choong PF. Percutaneous radiofrequency ablation for osteoid osteoma: experience with a new treatment. *Med J Aust* 2006; 184:563–565.
11. Schmidt D, Clasen S, Schaefer JF, et al. CT-guided radiofrequency (RF) ablation of osteoid osteoma: clinical long-term results. *Rofo* 2011; 183:381–387. [\[CrossRef\]](#)
12. Streitparth F, Gebauer B, Melcher I, et al. MR-guided laser ablation of osteoid osteoma in an open high-field system (1.0 T). *Cardiovasc Intervent Radiol* 2009; 32:320–325. [\[CrossRef\]](#)
13. Sequeiros RB, Hyvönen P, Sequeiros AB, et al. MR imaging-guided laser ablation of osteoid osteomas with use of optical instrument guidance at 0.23 T. *Eur Radiol* 2003; 13:2309–2314. [\[CrossRef\]](#)
14. Ronkainen J, Blanco Sequeiros R, Tervonen O. Cost comparison of low-field (0.23 T) MRI-guided laser ablation and surgery in the treatment of osteoid osteoma. *Eur Radiol* 2006; 16:2858–2865. [\[CrossRef\]](#)
15. Davies M, Cassar-Pullicino VN, Davies AM, et al. The diagnostic accuracy of MR imaging in osteoid osteoma. *Skeletal Radiol* 2002; 31:559–569. [\[CrossRef\]](#)
16. Lee MH, Ahn JM, Chung HW, et al. Osteoid osteoma treated with percutaneous radiofrequency ablation: MR imaging follow-up. *Eur J Radiol* 2007; 64:309–314. [\[CrossRef\]](#)
17. Campanacci M, Ruggieri P, Gasbarrini A, et al. Osteoid osteoma. Direct visual identification and intralesional excision of the nidus with minimal removal of bone. *J Bone Joint Surg Br* 1999; 81:814–820. [\[CrossRef\]](#)
18. Rosenthal DI, Springfield DS, Gebhardt MC, et al. Osteoid osteoma: percutaneous radio-frequency ablation. *Radiology* 1995; 197:451–454.
19. Sim FH, Dahlin CD, Beabout JW. Osteoid osteoma: diagnostic problems. *J Bone Joint Surg Am* 1975; 57:154–159.
20. Albisinni U, Rimondi E, Malaguti MC, et al. Radiofrequency thermoablation in the treatment of osteoid osteoma. *Radiology* 2004; 232:304–305. [\[CrossRef\]](#)
21. Martel J, Bueno A, Dominguez MP, et al. Percutaneous radiofrequency ablation: relationship between different probe types and procedure time on length and extent of osteonecrosis in dog long bones. *Skeletal Radiol* 2008; 37:147–152. [\[CrossRef\]](#)
22. Pinto CH, Taminiu AH, Vanderschueren GM, et al. Technical considerations in CT-guided radiofrequency thermal ablation of osteoid osteoma: tricks of the trade. *AJR Am J Roentgenol* 2002; 179:1633–1642.
23. Rybak LD, Gangi A, Buy X, et al. Thermal ablation of spinal osteoid osteomas close to neural elements: technical considerations. *AJR Am J Roentgenol* 2010; 195:293–298. [\[CrossRef\]](#)
24. Rimondi E, Mavrogenis AF, Rossi G, et al. Radiofrequency ablation for non-spinal osteoid osteomas in 557 patients. *Eur Radiol* 2012; 22:181–188. [\[CrossRef\]](#)

25. Goldberg SN, Grassi CJ, Cardella JF, et al. Image-guided tumor ablation: standardization of terminology and reporting criteria. *Radiology* 2005; 235:728–739. [\[CrossRef\]](#)
26. Lane MD, Le HB, Lee S, et al. Combination radiofrequency ablation and cementoplasty for palliative treatment of painful neoplastic bone metastasis: experience with 53 treated lesions in 36 patients. *Skeletal Radiol* 2011; 40:25–32. [\[CrossRef\]](#)
27. Zou KH, Tuncali K, Silverman SG. Correlation and simple linear regression. *Radiology* 2003; 227:617–622. [\[CrossRef\]](#)
28. Hadjipavlou AG, Tzermiadianos MN, Kakavelakis KN, Lander P. Percutaneous core excision and radiofrequency thermo-coagulation for the ablation of osteoid osteoma of the spine. *Eur J Spine* 2009; 18:345–351.
29. Vanderschueren GM, Taminiau AH, Obermann WR, et al. Osteoid osteoma: clinical results with thermocoagulation. *Radiology* 2002; 224:82–86. [\[CrossRef\]](#)
30. Cioni R, Armillotta N, Bargellini I, et al. CT-guided radiofrequency ablation of osteoid osteoma: long-term results. *Eur Radiol* 2004; 14:1203–1208. [\[CrossRef\]](#)
31. Donkol RH, Al-Nammi A, Moghazi K. Efficacy of percutaneous radiofrequency ablation of osteoid osteoma in children. *Pediatr Radiol* 2008; 38:180–185. [\[CrossRef\]](#)
32. Rimondi E, Bianchi G, Malaguti MC, et al. Radiofrequency thermoablation of primary non-spinal osteoid osteoma: optimization of the procedure. *Eur Radiol* 2005; 15:1393–1399. [\[CrossRef\]](#)
33. Rosenthal DI, Hornicek FJ, Torriani M, et al. Osteoid osteoma: percutaneous treatment with radiofrequency energy. *Radiology* 2003; 229:171–175. [\[CrossRef\]](#)
34. Mastrantuono D, Martorano D, Verna V, Mancini A, Faletti C. Osteoid osteoma: our experience using radio-frequency (RF) treatment. *Radio Med* 2005; 109:220–228. [\[CrossRef\]](#)
35. Mylona S, Patsoura S, Galani P, et al. Osteoid osteomas in common and in technically challenging locations treated with computed tomography-guided percutaneous radiofrequency ablation. *Skeletal Radiol* 2010; 39:443–449. [\[CrossRef\]](#)
36. Barei DP, Moreau G, Scarborough MT, et al. Percutaneous radiofrequency ablation of osteoid osteoma. *Clin Orthop Relat Res* 2000; 373:115–124. [\[CrossRef\]](#)
37. Vanderschueren GM, Taminiau AH, Obermann WR, et al. The healing pattern of osteoid osteomas on computed tomography and magnetic resonance imaging after thermocoagulation. *Skeletal Radiol* 2007; 36:813–821. [\[CrossRef\]](#)
38. Liu PT, Chivers FS, Roberts CC, et al. Imaging of osteoid osteoma with dynamic gadolinium-enhanced MR imaging. *Radiology* 2003; 227:691–700. [\[CrossRef\]](#)
39. Chai JW, Hong SH, Choi JY, et al. Radiologic diagnosis of osteoid osteoma: from simple to challenging findings. *Radiographics* 2010; 30:737–749. [\[CrossRef\]](#)
40. Klein MH, Shankman S. Osteoid osteoma: radiologic and pathologic correlation. *Skeletal Radiol* 1992; 21:23–31. [\[CrossRef\]](#)
41. Sofka CM, Saboeiro GR, Schneider R. Magnetic resonance imaging diagnosis and computed tomography-guided radiofrequency ablation of osteoid osteoma. *HSS J* 2006; 2:55–58. [\[CrossRef\]](#)
42. Cantwell CP, Kerr J, O’Byrne J, et al. MRI features after radiofrequency ablation of osteoid osteoma with cooled probes and impedance-control energy delivery. *AJR Am J Roentgenol* 2006; 186:1220–1227. [\[CrossRef\]](#)
43. Grey AC, Davies AM, Mangham DC, et al. The ‘penumbra sign’ on T1-weighted MR imaging in subacute osteomyelitis: frequency, cause and significance. *Clin Radiol* 1998; 53:587–592. [\[CrossRef\]](#)
44. Asch DA, Jedrzejewski MK, Christakis NA. Response rates to mail surveys published in medical journals. *J Clin Epidemiol* 1997; 50:1129–1136. [\[CrossRef\]](#)